

RSC Advances



This is an *Accepted Manuscript*, which has been through the Royal Society of Chemistry peer review process and has been accepted for publication.

Accepted Manuscripts are published online shortly after acceptance, before technical editing, formatting and proof reading. Using this free service, authors can make their results available to the community, in citable form, before we publish the edited article. This *Accepted Manuscript* will be replaced by the edited, formatted and paginated article as soon as this is available.

You can find more information about *Accepted Manuscripts* in the [Information for Authors](#).

Please note that technical editing may introduce minor changes to the text and/or graphics, which may alter content. The journal's standard [Terms & Conditions](#) and the [Ethical guidelines](#) still apply. In no event shall the Royal Society of Chemistry be held responsible for any errors or omissions in this *Accepted Manuscript* or any consequences arising from the use of any information it contains.

Synthesis, Insecticidal Activity, Structure–Activity Relationship (SAR) and Density Functional Theory (DFT) of Novel Anthranilic Diamides Analogs Containing 1,3,4-Oxadiazole Rings†

Cite this: DOI: 10.1039/x0xx00000x

Received 00th January 2014,

Accepted 00th January 2014

DOI: 10.1039/x0xx00000x

www.rsc.org/

Qi Liu,^a Kai Chen,^a Qiang Wang^a, Jueping Ni,^b Yufeng Li,^a Hongjun Zhu^{*a} and Yuan Ding^a

A series of anthranilic diamides analogs (**5a-x**) containing 1,3,4-oxadiazole rings were synthesized and characterized by ¹H NMR, ¹³C NMR and mass spectrometry. The structure of *N*-(4-chloro-2-methyl-6-(5-(thiophen-2-yl)-1,3,4-oxadiazol-2-yl)phenyl)methacrylamide (**5u**, CCDC 990869) was determined by X-ray diffraction crystallography. The insecticidal activities of these new compounds against diamondback moth (*Plutella xylostella*) were evaluated. Preliminary bioassays indicated that some of these compounds exhibited good insecticidal activities against *P. xylostella*, especially for 3-bromo-*N*-(4-bromo-2-methyl-6-(5-(pyrazin-2-yl)-1,3,4-oxadiazol-2-yl)phenyl)-1-(3-chloropyridin-2-yl)-1*H*-pyrazole-5-carboxamide (**5d**), which displayed 100 %, 80.95 % and 57.14 % activity against *P. xylostella* at 40 μg mL⁻¹, 10 μg mL⁻¹ and 4 μg mL⁻¹, respectively. The relationship between structure and insecticidal activity was discussed. The density functional theory (DFT) studies could be helpful to understand the various insecticidal activities.

Introduction

To discover a new type of environmental-friendly insecticide with high activity, low toxicity as well as low residue has become an urgent subject for science researchers. Recently, emergence of commercial insecticides that target insect ryanodine receptors, the anthranilic diamides (Chlorantraniliprole¹ Fig. 1a and Cyantraniliprole² Fig. 1b), have inaugurated a new era of synthetic insecticides. They exhibit exceptional broad-spectrum, high activity and low toxicity. Especially, chlorantraniliprole, the first anthranilic diamide insecticide, accounts for its low mammalian toxicity and favorable environmental profile.³ They act by activating the insect ryanodine receptor, which is a non-voltage-gated calcium channel to affect calcium release from intracellular stores by locking channels in a partially opened state, an assignment based on electrophysiological and Ca²⁺-release studies.^{4, 5} Owing to its prominent insecticidal activity, unique mode of action, and good environmental profiles, anthranilic diamide analogues have attracted more and more interest in this field. Generally, the chemical structure of anthranilic diamides could be characterized by three parts (Fig. 2a): aromatic bridge moiety (A), *N*-pyridylpyrazole amide moiety (B) and aliphatic amide moiety (C). In previous work, most modifications for chlorantraniliprole were related to Part (A)^{2, 6-8} and Part (B)⁹⁻¹⁴. As for Part (C), structural

modifications, such as cyano,¹⁵ hydrazone,¹⁶ and heterocyclic groups,¹⁷ were reported. Recently, a novel pyrazolecarboxamide with a thiadiazol group in the orthoposition (JS9117 Fig. 1c) was reported with high insecticidal activity.¹⁸ Compound d (Fig. 1d) containing an oxazoline group reported by Kang et al. showed good larvicidal activity against beet armyworm (*Spodoptera exigua*),¹⁹ indicating the Part (C) is attractive in further modification. Considering the inspired studies¹⁷⁻¹⁹ and bioisosterism²⁰, the aliphatic amide part (C) of anthranilic diamides could be concealed in the 1,3,4-oxadiazole ring (Fig. 2b) which is an efficient pharmacophore was extensively used in pesticide and drug molecule design.^{17, 21-23} In this way, we suggest that a high activity 1,3,4-oxadiazole, maybe the bioisostere of the aliphatic amide, is introduced into the *o*-heterocyclic phenylformamide structure, which might attain the satisfying activity. Thus it is worthy for us to explore the investigation.

According to the frontier molecular orbital theory, HOMO and LUMO are the two most important factors that affect the bioactivities of compounds.^{14, 24-27} It establishes correlation in various chemical and biochemical systems.^{28, 29} Recently, Zhengming Li research group^{14, 24, 26, 27} and Xing-hai Liu research group^{25, 30} reported study on the frontier orbital energy could provide useful information about the biological

mechanism. Thus, the DFT studies possibly could be used for the insecticidal activity investigating.

Taking all these into account, we successfully designed and synthesized a series of new anthranilic diamides derivatives containing 1,3,4-oxadiazole. The single crystal structure of one target compound has been verified, which could stimulate a better understanding of the binding nature of these compounds, and might help to explore new structures to enhance their biological activities. The larvicidal activities against *Plutella xylostella* (*P. xylostella*) were tested accordingly, and their preliminary structure–activity relationships were also discussed. Moreover, the DFT studies were used for the insecticidal activity investigating.

Results and discussion

Synthesis

The key intermediate **3** were synthesized from 2-amino-5-halo-3-methylbenzoic acid referring to the literature (Schemes 1, see ESI† for details).^{17,31}

The synthesis of final compounds **5** was accomplished by use of the pathway illustrated in Scheme 2. The condensation reaction of compound **3** with aromatic hydrazide compound in the presence of sodium hydroxide or potassium hydroxide, gave diacylhydrazine derivatives **4**. Once the formation of compounds **4** reached completeness, triethylamine (TEA) and 4-methylbenzenesulfonyl chloride (PTSC) were charged to afford the final compounds **5**.³²

Through our study, we find that a suitable dehydrating agent play an important role in the cyclodehydration reaction of diacylhydrazines derivatives **4**. Among the variety of available dehydrating agents, we tried trifluoroacetic anhydride (TFAA)³³ first, while their yields were less than 20 %. In addition, according to the literature,³² we chose PTSC, which is a non-toxic and cheap reagent. As was the case with the PTSC, the cyclodehydration reaction of diacylhydrazines derivatives **4** proceeded well at room temperature, giving isolated yields up to 85.2 % (Table 1).

Structure

The structures of all synthesized title compounds were confirmed by ¹H NMR, ¹³C NMR and mass spectrometry. The single peak appearing at the lowest field of δ 10.66–9.58 ppm in the ¹H NMR can be assigned to the aromatic amide hydrogen (-NH-C=O) of the target compounds. The chemical shift of Ph-CH₃ appears at δ 2.13–2.42. In addition, compound **5u** was recrystallized from dichloromethane to give colourless crystals (0.30 mm × 0.20 mm × 0.10 mm) suitable for X-ray single-crystal diffraction with the following crystallographic parameters: $a = 9.774(2)$ Å, $b = 9.830(2)$ Å, $c = 9.908(2)$ Å, $\alpha = 91.70(3)^\circ$, $\beta = 110.52(3)^\circ$ and $\gamma = 106.41(3)^\circ$. The detailed crystallographic data for **5u** can be found in the ESI† (Table S1). The single crystal structure diagram of **5u** is shown in Fig. 3. The bond lengths of possible intramolecular hydrogen bonds (H3C...N1, H8A...O1, H13A...O2 and H13A...N3) were 2.36

Å, 2.39 Å, 2.51 Å and 2.49 Å, respectively. And the intramolecular hydrogen bonds resulted in the formation of two planar pseudo rings A (C13/H13A/N3/C12/C11) and B (C8/H8A/O1/C6/C7), and two non-planar pseudo rings C (C13/H13A/O2/C14/N3/C12/C11) and D (N3/H3/N1/C6/C7/C12), which may be effective in the stabilization of the structure.³⁴ The bridge benzene ring (C7 to C12) and the terminal thiophene ring (C1/C2/C3/C4/S1) were connected with the 1,3,4-oxadiazole ring, which twisted 8.38° and 3.58° respectively and the three rings were almost located in the same plane. Meanwhile, in the molecular packing of **5u**, offset face-to-face π -stacking interactions between neighbouring molecular 1,3,4-oxadiazole units are observed in Fig. 3 and the intermolecular distance is 3.72 Å. These crystallographic data might provide the basis for elucidating the effect on their biological activities.

Biological activities and structure–activity relationships

The larvicidal activity of compounds **5a–x** and commercial chlorantraniliprole against *P. xylostella* is summarized in Tables 2. All of the compounds were initially tested at a concentration of 100 $\mu\text{g mL}^{-1}$, and consequently the compounds with high insecticidal potency were investigated further at low concentration. The bioassay results indicated that most of the compounds showed moderate to good insecticidal activities. Especially compounds **5d** and **5h** showed more than 57.14% and 52.38% larvicidal activities at the concentration of 4 $\mu\text{g mL}^{-1}$. Although it is difficult to found a specific structure–activity relationship from these data, it still shows the following general trend.

From Table 2, we can see that at the concentration of 100 $\mu\text{g mL}^{-1}$, *N*-pyridylpyrazole group substituted compounds **5a–h** showed 86.36–100 % larvicidal activities against *Plutella xylostella*, phenyl group substituted compounds **5i–p** exhibited 5.26–66.67 % activities, and isopropenyl group substituted compounds **5q–x** possessed 0.00–16.67 % activities, respectively. When the concentration of the test compounds was reduced to 10 $\mu\text{g mL}^{-1}$, most of *N*-pyridylpyrazole group substituted compounds (**5a–h**) can still exhibit better mortality against *P. xylostella*, for example, **5d** displayed 80.95% mortality, **5g** and **5h** possessed 71.43 % larvicidal activities. It revealed that the compounds with *N*-pyridylpyrazole can show much more remarkable mortality than the compounds with phenyl group or isopropenyl group. This may be due to the more hydrophobic nature of *N*-pyridylpyrazole group resulted in an appropriate overall log *P* value (around 5). Besides, the appropriate ionization constants (pK_a 10.60–10.65) which were close to the value of chlorantraniliprole (pK_a 10.77) also contributed to drug absorption.³⁵ To understand which substituent on the bridge benzene ring show more active in larvicidal activity, benzene ring was fixed as Cl or Br. As illustrated in Table 2, structure–activity relationship of all compounds, where X varied as Cl or Br, suggested the trend Cl \approx Br.

Moreover, to investigate the influence of different substitutions on the 1,3,4-oxadiazole ring, 2-thienyl group, phenyl group, 3-pyridyl group and 2-pyrazinyl group were introduced into R₂. Although it is hard to construct a clear structure–activity relationship from the data shown in Table 2, we can also conclude that the general trend in larvicidal is 2-pyrazinyl group > 3-pyridyl group > phenyl group > 2-thienyl group. For example, at the concentration of 10 µg mL⁻¹, compound **5a** (R₂=2-thienyl group, log *P*=6.60), **5b** (R₂= phenyl group, log *P*=6.62), **5c** (R₂=3-pyridyl group, log *P*=5.28) and **5d** (R₂=2-pyrazinyl group, log *P*=4.37) exhibited 47.62 %, 52.38 %, 57.14 % and 80.95 % activity against *P. xylostella* respectively. It revealed that the introduction of electron-withdrawing and weak hydrophobic substituents R₂ may contribute to the insecticidal activity increase against *P. xylostella*. In addition, when the concentration was reduced to 4 µg mL⁻¹ and 1 µg mL⁻¹, **5d** displayed 57.14 % and 38.10 % mortality. This result implied that 1,3,4-oxadiazole connected pyrazinyl group maybe a potential pharmacophore against *P. xylostella*.

DFT calculation

The frontier molecular orbitals play an important role in several chemical and pharmacological processes.³⁶ HOMO (Highest Occupied Molecular Orbital) has the priority to provide electrons, whereas LUMO (Lowest Unoccupied Molecular Orbital) accepts electrons first.^{37, 38} Thus, study of the frontier orbital may help for insecticidal activity investigating. Three compounds (**5a**, **5d** and **5t**) having relatively greater difference in activity were selected for DFT comparison.

The optimized geometry corresponding to the minimum on the potential energy surface has been obtained by solving self-consistent field equation iteratively. Generally, the compound **5a**, **5d** and **5t** showed that phenyl ring is not coplanar with 1,3,4-oxadiazole ring; while the R₂ group was nearly planar with the 1,3,4-oxadiazole ring. The pyridyl group showed a deviation from pyrazolyl group. The detailed geometrical parameters of the compounds calculated can be found in the ESI (Table S2–S4).

LUMO and HOMO Energies and HOMO–LUMO (H–L) Gaps (in eV) of **5a**, **5d** and **5t** are listed in Table 3. Compare the H–L gap of three molecules, the order was: **5t** > **5a** > **5d**. The narrow HOMO–LUMO gap implies a high chemical reactivity because it is energetically favorable to add electrons to a low-lying LUMO or extract electrons from a high-lying HOMO, and so to form an activated complex of any potential reaction.³⁹ This suggested that compound **5d** might possess relatively high activity, which correlated well with our experimental results. The HOMO and LUMO maps were shown in Fig. 4. In the HOMO of **5a**, **5d**, and **5t**, electrons are mainly delocalized on the benzene ring (including bromine atom), the amide bridge and 1,3,4-oxadiazole ring; in addition, electrons are also delocalized on R₁ and R₂ groups in varying degrees. When electron transitions take place, some electrons in the HOMO will enter into the LUMO;²⁶ then, in the LUMO of **5a**, **5d**, and **5t**, the electrons were similarly delocalized on three aromatic

rings (1,3,4-oxadiazole ring and two aromatic rings attached to it). The different electron distribution among **5a**, **5d**, and **5t** may possibly cause the large difference in larvicidal activity.

The amide bridge group can be observed in the HOMO maps of three molecules (**5a**, **5d**, and **5t**). the amide bridge can play an important role in the insecticidal activity through hydrophobic interaction.¹⁴ Although exact binding site(s) on insect ryanodine receptor have not been confirmed and are still unclear, researcher found hydrophobic C-terminal domain of the RyR I protein had a strong effect on the properties of the calcium release channel.⁴⁰ Thus, the distribution of the frontier orbitals may be related to the hydrophobic interaction of molecule with target receptor.

As Fig. 4 shown, in HOMO maps, three molecules showed different degrees of electron delocalization. The general trend according to electron delocalization was **5t** > **5a** > **5d**, which was negative correlation with their insecticidal activity. As reported,^{14, 24, 27} the frontier molecular orbitals are located on the main groups, the atoms of which can easily bind with the receptor. Moreover the different degrees of delocalization may affect the orbital interaction.⁴¹ Thus, it seemed that the high electron delocalization of **5t** or **5a** in HOMO may possibly make the orbital interactions limited, which may bring about the decrease in activity. And the orbital interactions between selected compounds (**5a**, **5d** and **5t**) and some side of residue chains of receptors might be dominated by hydrophobic interactions of the amide bridge among the frontier molecular orbitals.

Materials and methods

Analytical methods

Unless otherwise noted, reagents were purchased from commercial suppliers like Aladdin, Energy Chemical and Sinopharm Chemical Reagent Co., Ltd. And they were used without further purification while all solvents were redistilled before use. Analytical thin layer chromatography was performed on silica gel GF254. Silica gel (200–300 mesh) was used for flash column chromatography. Melting points (mp) were taken on an X-4 microscope electrothermal apparatus (Taikhe China) and are uncorrected. The nuclear magnetic resonance (¹H NMR and ¹³C NMR) spectra were recorded on a Bruker AV-100 spectrometer at 100 MHz or a Bruker AV-400 spectrometer at 400 MHz, using CDCl₃ or DMSO-*d*₆ as the solvent, with tetramethylsilane (TMS) as an internal standard. Mass spectra were recorded with an Agilent 1100 Series LC/MSD Trap SL. The synthetic procedures and detailed characterization data of intermediates **3a–f** and different amidoximes can be found in the ESI. †

Chemical synthesis

General procedure for the synthesis of compounds 5a-x

A mixture of **3a–f** (20.0 mmol), solid aromatic hydrazide compound (24.0 mmol) and *N,N*-dimethylformamide (100 mL)

was stirred at r.t. for 15 min. Then solid sodium hydroxide (10.0 mmol) was added into the solution. Once the formation of intermediates **4a-x** reached completeness, more liquid triethylamine (2 equiv) and solid 4-methylbenzenesulfonyl chloride (3 equiv) were charged to afford the pyrazinyl group substituted 1,3,4-oxadiazole rings. The mixture was poured into 500 mL saturated sodium bicarbonate solution. The solid was filtered, washed with water, and dried to afford solid **5a-x**. The crude product was purified by flash chromatography.

X-ray diffraction crystallography

A suitable single crystal of compound **5u** (CCDC 990869) was obtained by dissolving the compound in dichloromethane and evaporating the solvent slowly at r.t. for about 7 d. The diffraction data were collected on a Nonius CAD4 single crystal diffractometer with graphite-monochromated MoK α radiation ($\lambda = 0.71073 \text{ \AA}$) by using a $\omega/2\theta$ scan mode at 293 K. The crystal structure was solved by the direct method and refined by the full-matrix least-squares procedure on F² using SHELXL-97 program.⁴² All non-hydrogen atoms were refined anisotropically, and the hydrogen atoms were introduced at calculated positions.

Insecticidal activities assay

The larvicidal activities of the title compounds (**5a-x**) against *Plutella xylostella* were evaluated by a dipping method according to the literature procedures.⁴³ Cabbage leaf disks (8 cm in diameter) were dipped into a test solution for 10 s and air-dried on filter paper. The treated diet was released into the petri dish, and twenty one third-instar *P. xylostella* were released into the petri dish. *P. xylostella* affected by this treatment were assessed for 3 days after the treatment.

P. xylostella with abnormal symptoms such as body contraction, feeding cessation, or paralysis were included in the number of dead.⁴³ The results are listed in Table 1, in which the mortality percentage was expressed as the mean of values obtained in three independent experiments. Chlorantraniliprole, the lead compound, was used as a control.

Computational methods

The structures of compounds **5a**, **5d** and **5t** were selected as the initial structures, whereas the DFT-B3LYP/6-31G*⁴⁴⁻⁵⁰ method in the Gaussian 09⁵¹ package was used to optimized structures were in accordance with the minimum points on the potential energy surfaces. pK_a was predicted by using ACD/labs version 6.0.⁵² Log *P* (*n*-octanol/water partition coefficients) was predicted by using ChemBioOffice Ultra version 12.0 from CambridgeSoft Corporation.⁵³ All of the calculations were carried out on the supercomputer in Nanjing Tech University.

Conclusions

In summary, a series of new anthranilic diamide analogs containing substituted 1,3,4-oxadiazole ring were designed and synthesized. Preliminary bioassays indicated that some of the

compounds showed good larvicidal activities against *P. xylostella*. In particular, compounds **5d** against *P. xylostella* were 57.14 % and 38.10 % activity at 4 $\mu\text{g mL}^{-1}$ and 1 $\mu\text{g mL}^{-1}$, respectively. The preliminary structure-activity relationship (SAR) of the title compounds indicated that compound attached *N*-pyridylpyrazole showed much more remarkable mortality than compound attached phenyl group or isopropenyl group. Furthermore, the compounds with electron-withdrawing and weak hydrophobic substituents on 1,3,4-oxadiazole ring can display better insecticidal activity than others. And through density functional theory (DFT) studies, it seemed that the high electron delocalization of **5t** or **5a** in HOMO may possibly make the orbital interactions limited, which may bring about the decrease in activity. And the orbital interactions between selected compounds (**5a**, **5d** and **5t**) and some side of residue chains of receptors might be dominated by hydrophobic interactions among the frontier molecular orbitals. With the expectation of finding more new 1,3,4-oxadiazole containing anthranilic diamide analogs, further structural optimization and larvicidal activity tests are under way.

Acknowledgements

This work is financially by the National key technology R&D program of the Ministry of Science and Technology (2011BAE06B01-11), the Technology R&D Program of Jiangsu province (BE2012363), the Postgraduate innovation fund of Jiangsu province (2013, CXLX13_399).

We thank Jiangsu Pesticide Research Institute Co., Ltd. for the test of biological activities.

Notes and references

^a Department of Applied Chemistry, College of Science, Nanjing Tech University, Nanjing 211816, P. R. China. E-mail: zhu hj@njtech.edu.cn; Fax: +86 25 83587443; Tel: +86 25 83172358

^b Jiangsu Pesticide Research Institute Co Ltd., Nanjing 210047, P. R. China.

† Electronic Supplementary Information (ESI) available: Characterization data of compounds **5a-x**, general synthetic methods and schemes for intermediates **3a-f**, crystal and structure refinement data of compound **5u**, ¹H NMR spectra and mass spectra for all target compounds **5a-x**, and the data for DFT calculation. **CCDC 990869**

See DOI: 10.1039/b000000x/

1. G. P. Lahm, T. P. Selby, J. H. Freudenberger, T. M. Stevenson, B. J. Myers, G. Seburyamo, B. K. Smith, L. Flexner, C. E. Clark and D. Cordova, *Bioorg. Med. Chem. Lett.*, 2005, **15**, 4898-4906.
2. *WO. Pat.*, 2004067528, 2004.
3. M. Luo, Q. Chen, J. Wang, C. Hu, J. Lu, X. Luo and D. Sun, *Bioorg. Med. Chem. Lett.*, 2014, **24**, 1987-1992.
4. D. Cordova, E. A. Benner, M. D. Sacher, J. J. Rauh, J. S. Sopa, G. P. Lahm, T. P. Selby, T. M. Stevenson, L. Flexner, S. Gutteridge, D.

- F. Rhoades, L. Wu, R. M. Smith and Y. Tao, *Pestic. Biochem. Physiol.*, 2006, **84**, 196-214.
5. Y. Li, M. Mao, Y. Li, L. Xiong, Z. Li and J. Xu, *Physiol. Entomol.*, 2011, **36**, 230-234.
6. *WO. Pat.*, 2009024341, 2009.
7. C. Gnamm, A. Jeanguenat, A. C. Dutton, C. Grimm, D. P. Kloer and A. J. Crossthwaite, *Bioorg. Med. Chem. Lett.*, 2012, **22**, 3800-3806.
8. *WO. Pat.*, 2007093402, 2007.
9. X. Zhang, Y. Li, J. Ma, H. Zhu, B. Wang, M. Mao, L. Xiong, Y. Li and Z. Li, *Bioorg. Med. Chem.*, 2014, **22**, 186-193.
10. Y. Zhao, Y. Li, L. Xiong, H. Wang and Z. Li, *Chin. J. Chem.*, 2012, **30**, 1748-1758.
11. Z. Liu, Q. Feng, L. Xiong, M. Wang and Z. Li, *Chin. J. Chem.*, 2010, **28**, 1757-1760.
12. *WO. Pat.*, 2006000336, 2006.
13. Q. Feng, Z. L. Liu, L. X. Xiong, M. Z. Wang, Y. Q. Li and Z. M. Li, *J. Agric. Food Chem.*, 2010, **58**, 12327-12336.
14. B. L. Wang, H. W. Zhu, Y. Ma, L. X. Xiong, Y. Q. Li, Y. Zhao, J. F. Zhang, Y. W. Chen, S. Zhou and Z. M. Li, *J. Agric. Food Chem.*, 2013, **61**, 5483-5493.
15. M. Mao, Y. Li, Q. Liu, Y. Zhou, X. Zhang, L. Xiong, Y. Li and Z. Li, *Bioorg. Med. Chem. Lett.*, 2013, **23**, 42-46.
16. J. Wu, B. A. Song, D. Y. Hu, M. Yue and S. Yang, *Pest Manage. Sci.*, 2012, **68**, 801-810.
17. Y. Li, H. Zhu, K. Chen, R. Liu, A. Khallaf, X. Zhang and J. Ni, *Org. Biomol. Chem.*, 2013, **11**, 3979-3988.
18. *WO. Pat.*, 2011085575, 2011.
19. *CN. Pat.*, 101863884, 2010.
20. L. M. Lima and E. J. Barreiro, *Curr. Med. Chem.*, 2005, **12**, 23-49.
21. A. S. Aboraia, H. M. Abdel-Rahman, N. M. Mahfouz and M. A. El-Gendy, *Bioorg. Med. Chem.*, 2006, **14**, 1236-1246.
22. Z. Fan, Z. Shi, H. Zhang, X. Liu, L. Bao, L. Ma, X. Zuo, Q. Zheng and N. Mi, *J. Agric. Food Chem.*, 2009, **57**, 4279-4286.
23. N. Tabanca, A. Ali, U. R. Bernier, I. A. Khan, B. Kocyigit-Kaymakcioglu, E. E. Oruc-Emre, S. Unsalan and S. Rollas, *Pest Manage. Sci.*, 2013, **69**, 703-708.
24. X. H. Liu, P. Q. Chen, B. L. Wang, Y. H. Li, S. H. Wang and Z. M. Li, *Bioorg. Med. Chem. Lett.*, 2007, **17**, 3784-3788.
25. N. B. Sun, J. Q. Fu, J. Q. Weng, J. Z. Jin, C. X. Tan and X. H. Liu, *Molecules*, 2013, **18**, 12725-12739.
26. X. H. Liu, W. G. Zhao, B. L. Wang and Z. M. Li, *Res. Chem. Intermed.*, 2012, **38**, 1999-2008.
27. X. H. Liu, L. Pan, C. X. Tan, J. Q. Weng, B. L. Wang and Z. M. Li, *Pestic. Biochem. Phys.*, 2011, **101**, 143-147.
28. D. F. V. Lewis, C. Ioannides and D. V. Parke, *Xenobiotica*, 1994, **24**, 401-408.
29. Z. Zhou and R. G. Parr, *J. Am. Chem. Soc.*, 1990, **112**, 5720-5724.
30. G. X. Sun, H. K. Wu, M. Y. Yang, Z. H. Sun, X. H. Liu, Y. X. Shi, B. J. Li and Y. G. Zhang, *Int J Mol Sci*, 2014, **15**, 8075-8090.
31. N. Allendoerfer, M. Es-Sayed, M. Nieger and S. Brase, *Tetrahedron Lett.*, 2012, **53**, 388-391.
32. P. Stabile, A. Lamonica, A. Ribecai, D. Castoldi, G. Guercio and O. Curcuruto, *Tetrahedron Lett.*, 2010, **51**, 4801-4805.
33. S. Liras, M. P. Allen and B. E. Segelstein, *Synth. Commun.*, 2000, **30**, 437-443.
34. M. L. Feng, Y. F. Li, H. J. Zhu, L. Zhao, B. B. Xi and J. P. Ni, *J. Agric. Food Chem.*, 2010, **58**, 10999-11006.
35. M. Meloun and S. Bordovska, *Anal. Bioanal. Chem.*, 2007, **389**, 1267-1281.
36. Y. L. Ma, R. J. Zhou, X. Y. Zeng, Y. X. An, S. S. Qiu and L. J. Nie, *J. Mol. Struct.*, 2014, **1063**, 226-234.
37. A. A. Al-Amiery, R. I. Al-Bayati, F. M. Saed, W. B. Ali, A. A. H. Kadhum and A. B. Mohamad, *Molecules*, 2012, **17**, 10377-10389.
38. A. M. Mansour, *Inorg. Chim. Acta.*, 2013, **394**, 436-445.
39. Q. Wang, H. Wang, L. Wei, S. W. Yang and Y. Chen, *J. Phys. Chem. C*, 2012, **116**, 11709-11717.
40. N. Tilgen, F. Zorzato, B. Halliger-Keller, F. Muntoni, C. Sewry, L. M. Palmucci, C. Schneider, E. Hauser, F. Lehmann-Horn, C. R. Müller and S. Treves, *Hum. Mol. Genet.*, 2001, **10**, 2879-2887.
41. J. K. Cho and S. Shaik, *J. Am. Chem. Soc.*, 1991, **113**, 9890-9891.
42. G. Sheldrick, *SHELXL-97. Program for the Refinement of Crystal Structures*, University of Göttingen, Germany, 1997.
43. M. Tohnishi, H. Nakao, T. Furuya, A. Seo, H. Kodama, K. Tsubata, S. Fujioka, H. Kodama, T. Hirooka and T. Nishimatsu, *J. Pestic. Sci. (Tokyo, Jpn.)*, 2005, **30**, 354-360.
44. R. Krishnan, J. S. Binkley, R. Seeger and J. A. Pople, *J. Chem. Phys.*, 1980, **72**, 650-654.
45. T. Clark, J. Chandrasekhar, G. W. Spitznagel and P. v. R. Schleyer, *J. Comput. Chem.*, 1983, **4**, 294-301.
46. A. D. Becke, *J. Chem. Phys.*, 1993, **98**, 5648-5652.
47. P. C. Hariharan and J. A. Pople, *Theoret. Chim. Acta (Berl.)*, 1973, **28**, 213-222.
48. P. M. W. Gill, B. G. Johnson, J. A. Pople and M. J. Frisch, *Chem. Phys. Lett.*, 1992, **197**, 499-505.
49. M. M. Francl, W. J. Pietro, W. J. Hehre, J. S. Binkley, M. S. Gordon, D. J. DeFrees and J. A. Pople, *J. Chem. Phys.*, 1982, **77**, 3654-3665.
50. C. Lee, W. Yang and R. G. Parr, *Phys. Rev. B*, 1988, **37**, 785-789.
51. M. J. Frisch, G. W. Trucks, H. B. Schlegel, G. E. Scuseria, M. A. Robb, J. R. Cheeseman, G. Scalmani, V. Barone, B. Mennucci, G. A. Petersson, H. Nakatsuji, M. Caricato, X. Li, H. P. Hratchian, A. F. Izmaylov, J. Bloino, G. Zheng, J. L. Sonnenberg, M. Hada, M. Ehara, K. Toyota, R. Fukuda, J. Hasegawa, M. Ishida, T. Nakajima, Y. Honda, O. Kitao, H. Nakai, T. Vreven, J. A. Montgomery, Jr., J. E. Peralta, F. Ogliaro, M. Bearpark, J. J. Heyd, E. Brothers, K. N. Kudin, V. N. Staroverov, R. Kobayashi, J. Normand, K. Raghavachari, A. Rendell, J. C. Burant, S. S. Iyengar, J. Tomasi, M. Cossi, N. Rega, J. M. Millam, M. Klene, J. E. Knox, J. B. Cross, V. Bakken, C. Adamo, J. Jaramillo, R. Gomperts, R. E. Stratmann, O. Yazyev, A. J. Austin, R. Cammi, C. Pomelli, J. Ochterski, R. L. Martin, K. Morokuma, V. G. Zakrzewski, G. A. Voth, P. Salvador, J. J. Dannenberg, S. Dapprich, A. D. Daniels, O. Farkas, J. B. Foresman, J. V. Ortiz, J. Cioslowski and D. J. Fox, *GAUSSIAN 09 (Revision A.2)*, Gaussian, Inc., Wallingford, CT, 2009.
52. Advanced Chemistry Development, Inc., *ACD/pKa DB, Version 6.0*, Toronto, Ontario, Canada, 2001.
53. H. Lin, T. Annamalai, P. Bansod, Y.-C. Tse-Dinh and D. Sun, *Med. Chem. Commun.*, 2013, **4**, 1613-1618.

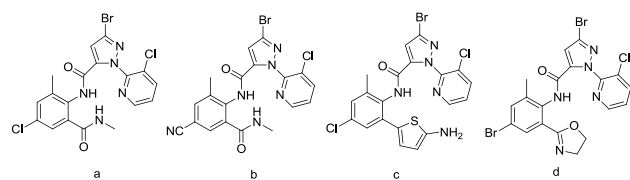


Fig. 1 Chemical structures of compounds a-e.

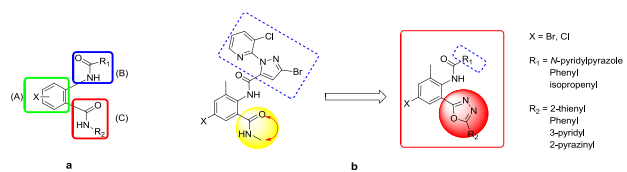


Fig. 2 General structure of anthranilic diamides and design strategy of the target compounds.

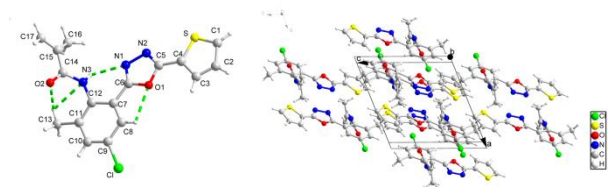


Fig. 3 Molecular structure of **5u** obtained from X-ray crystallography.

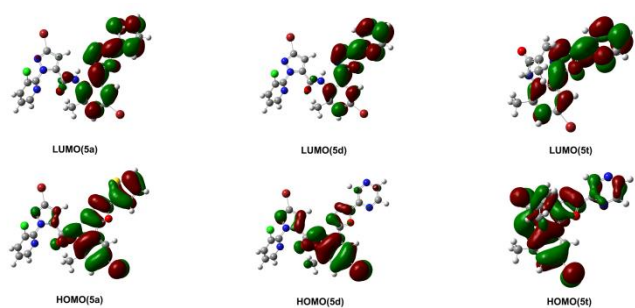
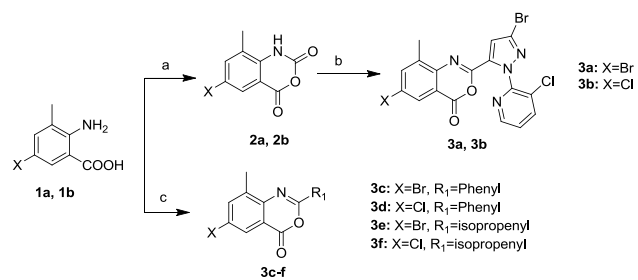
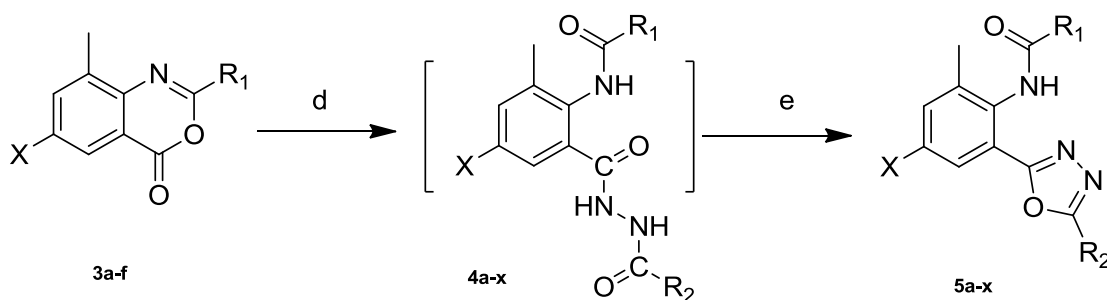


Fig. 3 LUMO and HOMO maps for compounds **5a**, **5d** and **5t** from DFT calculations. The green parts represent positive molecular orbital, and the red parts represent negative molecular orbital.



Scheme 1 Reagents and conditions: (a) ClCOOEt, Dioxane, reflux, ClCOCH₃, 55 °C; (b) 3-bromo-1-(3-chloropyridin-2-yl)-1H-pyrazole-5-carbonyl chloride, anhydrous pyridine, anhydrous acetonitrile, 60 °C; (c) Methacrylic anhydride/Benzoic anhydride, Pyridine, reflux.



5a: X=Br, R_1 =N-pyridylpyrazole, R_2 =2-thienyl
5b: X=Br, R_1 =N-pyridylpyrazole, R_2 =Phenyl
5c: X=Br, R_1 =N-pyridylpyrazole, R_2 =3-pyridyl
5d: X=Br, R_1 =N-pyridylpyrazole, R_2 =pyrazinyl
5e: X=Cl, R_1 =N-pyridylpyrazole, R_2 =2-thienyl
5f: X=Cl, R_1 =N-pyridylpyrazole, R_2 =Phenyl
5g: X=Cl, R_1 =N-pyridylpyrazole, R_2 =3-pyridyl
5h: X=Cl, R_1 =N-pyridylpyrazole, R_2 =pyrazinyl

5i: X=Br, R_1 =Phenyl, R_2 =2-thienyl
5j: X=Br, R_1 =Phenyl, R_2 =Phenyl
5k: X=Br, R_1 =Phenyl, R_2 =3-pyridyl
5l: X=Br, R_1 =Phenyl, R_2 =pyrazinyl
5m: X=Cl, R_1 =Phenyl, R_2 =2-thienyl
5n: X=Cl, R_1 =Phenyl, R_2 =Phenyl
5o: X=Cl, R_1 =Phenyl, R_2 =3-pyridyl
5p: X=Cl, R_1 =Phenyl, R_2 =pyrazinyl

5q: X=Br, R_1 =isopropenyl, R_2 =2-thienyl
5r: X=Br, R_1 =isopropenyl, R_2 =Phenyl
5s: X=Br, R_1 =isopropenyl, R_2 =3-pyridyl
5t: X=Br, R_1 =isopropenyl, R_2 =pyrazinyl
5u: X=Cl, R_1 =isopropenyl, R_2 =2-thienyl
5v: X=Cl, R_1 =isopropenyl, R_2 =Phenyl
5w: X=Cl, R_1 =isopropenyl, R_2 =3-pyridyl
5x: X=Cl, R_1 =isopropenyl, R_2 =pyrazinyl

Scheme 2 Reagents and conditions: (d) $R_2\text{CONHNH}_2$, NaOH, DMF, r.t.; (e) Et_3N , PTSC, DMF, r.t.

Table 1 The yields of compounds **5a-x**.

Cmpd.	Yield (%)	Cmpd.	Yield (%)	Cmpd.	Yield (%)
5a	80.4	5i	62.2	5q	47.2
5b	40.7	5j	43.5	5r	46.9
5c	73.0	5k	47.9	5s	20.7
5d	51.3	5l	61.6	5t	46.1
5e	77.2	5m	63.8	5u	45.1
5f	85.2	5n	51.2	5v	33.7
5g	67.1	5o	42.1	5w	28.3
5h	44.8	5p	31.7	5x	37.2

Table 2 Larvicidal activity against *P. xylostella* and physicochemical properties of compounds **5a-x**.

Cmpd.	X	R ₁	R ₂	p <i>K</i> _a ^a	Log <i>P</i> ^b	larvicidal activity 3d (%) at				
						100 µg mL ⁻¹	40 µg mL ⁻¹	10 µg mL ⁻¹	4 µg mL ⁻¹	1 µg mL ⁻¹
5a	Br	<i>N</i> -pyridylpyrazole	2-thienyl	10.65	6.60	100.00	76.19	47.62	19.05	4.76
5b	Br	<i>N</i> -pyridylpyrazole	Phenyl	10.66	6.62	100.00	85.71	52.38	28.57	4.76
5c	Br	<i>N</i> -pyridylpyrazole	3-pyridyl	10.63	5.28	90.00	77.78	57.14	28.57	23.81
5d	Br	<i>N</i> -pyridylpyrazole	2-pyrazinyl	10.60	4.37	100.00	100.00	80.95	57.14	38.10
5e	Cl	<i>N</i> -pyridylpyrazole	2-thienyl	10.65	6.33	86.36	76.19	23.81	0.00	0.00
5f	Cl	<i>N</i> -pyridylpyrazole	Phenyl	10.66	6.35	100.00	95.45	60.00	4.76	0.00
5g	Cl	<i>N</i> -pyridylpyrazole	3-pyridyl	10.63	5.01	100.00	100.00	71.43	9.52	4.76
5h	Cl	<i>N</i> -pyridylpyrazole	2-pyrazinyl	10.60	4.10	100.00	100.00	71.43	52.38	4.76
5i	Br	Phenyl	2-thienyl	11.84	5.37	5.56	/	0.00	/	/
5j	Br	Phenyl	Phenyl	11.85	5.39	18.75	/	0.00	/	/
5k	Br	Phenyl	3-pyridyl	11.82	4.05	16.67	/	0.00	/	/
5l	Br	Phenyl	2-pyrazinyl	11.79	3.14	28.57	/	0.00	/	/
5m	Cl	Phenyl	2-thienyl	11.84	5.10	5.26	/	0.00	/	/
5n	Cl	Phenyl	Phenyl	11.85	5.12	16.67	/	4.76	/	/
5o	Cl	Phenyl	3-pyridyl	11.82	3.78	47.62	/	4.76	/	/
5p	Cl	Phenyl	2-pyrazinyl	11.79	2.87	66.67	/	0.00	/	/
5q	Br	isopropenyl	2-thienyl	12.08	4.51	4.76	/	0.00	/	/
5r	Br	isopropenyl	Phenyl	12.10	4.53	4.76	/	0.00	/	/
5s	Br	isopropenyl	3-pyridyl	12.07	3.19	0.00	/	0.00	/	/
5t	Br	isopropenyl	2-pyrazinyl	12.03	2.28	18.75	/	4.76	/	/
5u	Cl	isopropenyl	2-thienyl	12.08	4.24	9.52	/	0.00	/	/
5v	Cl	isopropenyl	Phenyl	12.10	4.26	0.00	/	0.00	/	/
5w	Cl	isopropenyl	3-pyridyl	12.07	2.92	16.67	/	4.76	/	/
5x	Cl	isopropenyl	2-pyrazinyl	12.03	2.00	4.76	/	0.00	/	/
Chlorantraniliprole				10.77	4.26	100.00	100.00	100.00	100.00	100.00

^a calculated p*K*_a was predicted by using ACD/labs version 6.0.^b calculated Log *P* (*n*-octanol/water partition coefficients) was predicted by using ChemBioOffice Ultra version 12.0 from CambridgeSoft Corporation.

Table 3 LUMO and HOMO Energies and HOMO–LUMO (H–L) Gaps (in eV) of 5a, 5d and 5t.

	R ₁	R ₂	HOMO	LUMO	H-L Gaps
5a	<i>N</i> -pyridylpyrazole	2-thienyl	-6.30	-2.16	4.14
5d	<i>N</i> -pyridylpyrazole	2-pyrazinyl	-6.47	-2.53	3.94
5t	isopropenyl	2-pyrazinyl	-6.53	-2.32	4.21